Vortex lattice formation in a rotating Bose-Einstein condensate

Makoto Tsubota,[1] Kenichi Kasamatsu,[1] and Masahito Ueda[2]

[1]*Department of Physics, Osaka City University, Sumiyoshi-Ku, Osaka 558-8585, Japan*
[2]*Department of Physics, Tokyo Institute of Technology, Meguro-ku, Tokyo 152-8551, Japan*

We study the dynamics of vortex lattice formation of a rotating trapped Bose-Einstein condensate by numerically solving the two-dimensional Gross-Pitaevskii equation, and find that the condensate undergoes elliptic deformation, followed by unstable surface-mode excitations before forming a quantized vortex lattice. The origin of the peculiar surface-mode excitations is identified to be phase fluctuations at the low-density surface regime. The obtained dependence of a distortion parameter on time and that on the driving frequency agree with the recent experiments by Madison *et al.* [Phys. Rev. Lett. **86**, 4443 (2001)].

Quantized vortices have long been studied in superfluid ^{4}He as the topological defects characteristic of superfluidity [1,2]. However, the relatively high density and strong repulsive interaction complicate the theoretical treatments of the Bose-Einstein condensed liquid, and the healing length of the atomic scale makes the experimental visualization of the quantized vortices difficult. The recent achievement of Bose-Einstein condensation in trapped alkali-metal atomic gases at ultralow temperatures has stimulated intense experimental and theoretical activity. The atomic Bose-Einstein condensates (BECs) have the weak interaction because they are dilute gases, thus being free of the above difficulties that superfluid ^{4}He is subject to. Quantized vortices in the atomic BECs have recently been created experimentally by Mathews *et al.* [3], Madison *et al.* [4], and Abo-Shaeer *et al.* [5].

By rotating an asymmetric trapping potential, Madison *et al.* at ENS succeeded in forming a quantized vortex in ^{87}Rb BEC for a stirring frequency that exceeds a critical value [4]. Vortex lattices were obtained for higher frequencies. The ENS group subsequently observed that vortex nucleation occurs via a dynamical instability of the condensate [6]. For a given modulation amplitude and stirring frequency, the steady state of the condensate was distorted to an elliptic cloud, stationary in the rotating frame, as predicted by Recati *et al.* [7]. An intrinsic dynamical instability [8] of the steady state transformed the elliptic state into a more axisymmetric state with vortices. However, the origin of that instability and how it leads to the formation of vortex lattices remains to be investigated

The ENS group found that the minimum rotation frequency Ω_{nuc} at which one vortex appears is $0.65\omega_\perp$, where $\omega_\perp$ is the transverse oscillation frequency of the cigar-shaped trapping potential, independent of the number of atoms or the longitudinal frequency ω_z [9]. There is a discrepancy between the observations and the theoretical considerations based on the stationary solution of the Gross-Pitaevskii equation (GPE) [10,11]; Ω_{nuc} is significantly larger than its equilibrium estimates.

The present paper addresses these issues by numerically solving the GPE that governs the time evolution of the order parameter $\psi(\mathbf{r},t)$

$$(i-\gamma)\hbar\frac{\partial\psi}{\partial t}=\left[-\frac{\hbar^2}{2m}\nabla^2+V_{\mathrm{tr}}+g|\psi|^2-\mu-\Omega L_z\right]\psi. \quad (1)$$

Here, $g=4\pi\hbar^2 a/m$ is the coupling constant, proportional to the ^{87}Rb scattering length $a\approx5.77$ nm. The high anisotropy of the cigar-shaped potential used in the ENS experiments ($\omega_\perp/\omega_z\sim14$) may permit the two-dimensional analysis. We thus focus on the two-dimensional dynamics of Eq. (1) by assuming the trapping potential

$$V_{\mathrm{tr}}(\mathbf{r})=\frac{1}{2}m\omega_\perp^2\{(1+\epsilon_x)x^2+(1+\epsilon_y)y^2\}, \quad (2)$$

where $\omega_\perp=2\pi\times219$ Hz, and the parameters $\epsilon_x=0.03$ and $\epsilon_y=0.09$ describe small deviations of the trap from the axisymmetry, corresponding to the ENS experiments [4]. The centrifugal term $-\Omega L_z=i\hbar\Omega(x\partial_y-y\partial_x)$ appears in a system rotating about the z axis at a frequency Ω. An important characteristic parameter of the two-dimensional system is $C=8\pi Na/L$, with the total number N of the condensate atoms and L the size of the system along the z axis.

The term with γ in Eq. (1) introduces the dissipation. Although the detailed mechanism of the dissipation is yet to be understood, we include this term in the GPE because of the following reasons. First, collective damped oscillations of the condensate have been observed by Jin *et al.* and Mewes *et al.* [12], which shows the presence of some dissipative mechanisms and is consistent with the solution of the GPE with the dissipative term [13]. Second, even if the trapping potential is rotated fast enough, vortex lattices will never be formed without dissipation, because vortex lattice correspond to local minimum of the total energy in the configuration space [14]. In other words, the observation of the vortex lattices [4] implies the presence of dissipation. Following Ref. [13], we use $\gamma=0.03$ throughout this work.

In this paper, we focus on two kinds of responses of the condensate, namely, the response to the sudden turn on of the rotation of the potential, and that to the slow turn on. The numerical calculations are performed with the implicit Crank-Nicolson method. The chemical potential μ is adjusted at all times so as to preserve the number of condensate atoms.
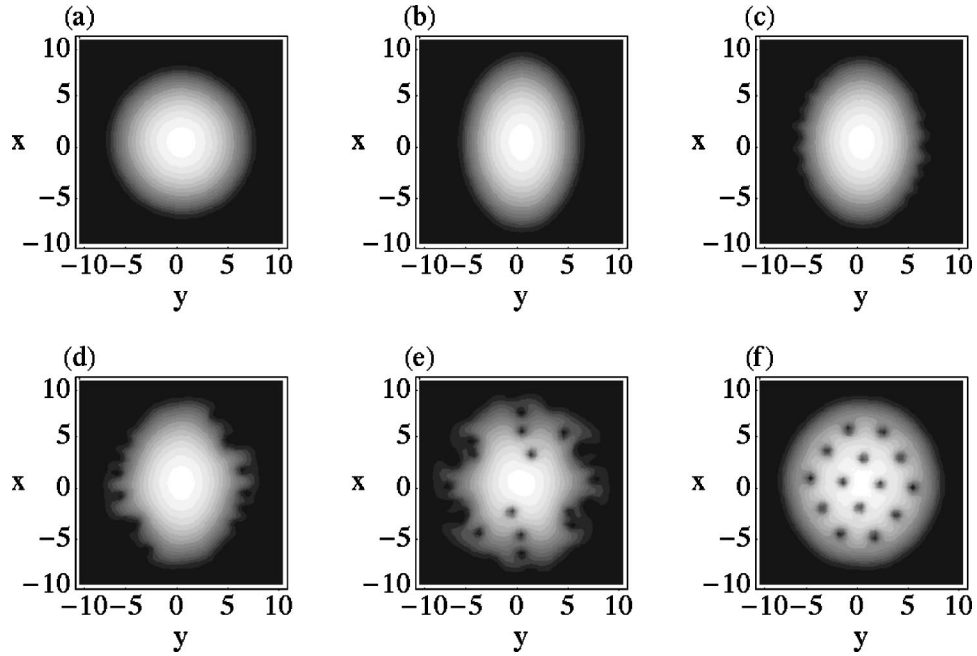
FIG. 1. Time development of the condensate density $|\psi|^2$ after the trapping potential begins to rotate suddenly with $\Omega=0.7\omega_\perp$. The time is $t=0$ msec (a), 21 msec (b), 107 msec (c), 114 msec (d), 123 msec (e), and 262 msec (f). The unit for length is $a_{\mathrm{HO}}=\sqrt{\hbar/2m\omega_\perp}=0.512$ μm and the period of the trap 4.57 msec.

We first prepare an equilibrium condensate with $C=1400$ trapped in a stationary potential. Figure 1 shows the typical dynamics of the condensate density $|\psi(\mathbf{r},t)|^2$ after the potential begins to rotate suddenly with $\Omega=0.7\omega_\perp$ [15]. The condensate is elongated along the x axis because of the small anisotropy of V_{tr} [Eq. (2)], and the elliptic cloud oscillates. Then, the boundary surface of the condensate becomes unstable, exciting the surface waves, which propagate along the surface. The excitations are likely to occur on the surface whose curvature is low, i.e., parallel to the longer axis of the ellipse. The ripples on the surface develop into the vortex cores around which superflow circulates. Subject to the dissipative vortex dynamics, some vortices enter the condensate, forming a vortex lattice. As the vortex lattice is being formed, the axial symmetry of the condensate is recovered by transferring angular momentum into quantized vortices.

This peculiar dynamics is understood by investigating the phase of $\psi(\mathbf{r},t)$ as shown in Fig. 2. There are some lines where the phase changes discontinuously from black to white, which corresponds to the branch cuts between the phases 0 and 2π. Their ends represent phase defects, i.e., vortices. As soon as the rotation starts, some defects begin to enter. When the defects are on the outskirts of the condensate where the amplitude $|\psi(\mathbf{r},t)|$ is almost negligible, they neither contribute to the energy nor the angular momentum of the system. These defects come into the boundary surface of the condensate within which the amplitude grows up. Then, the defects compete with each other and induce the above surface waves due to interference. There the selection of the defects starts, because their further invasion into the condensate costs the energy and the angular momentum. As is well known in the study of rotating superfluid helium [14], the rotating drive pulls vortices into the rotation axis, while repulsive interaction tends to push them apart; this competition yields a vortex lattice whose vortex density depends on the rotation frequency. In our case, some vortices enter the condensate and form a lattice dependent on Ω, while excessive
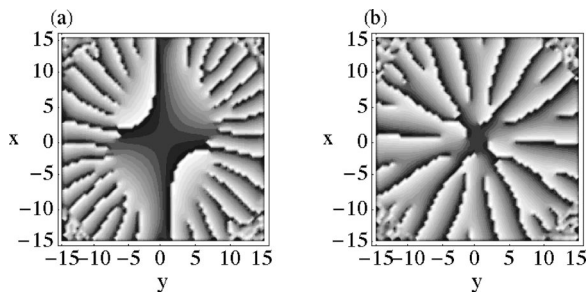

FIG. 2. Phase profile of ψ: (a) and (b) correspond to Figs. 1(c) and 1(f). The value of the phase varies continuously from 0 (black) to 2π (white). The unit for length is the same as that of Fig. 1.
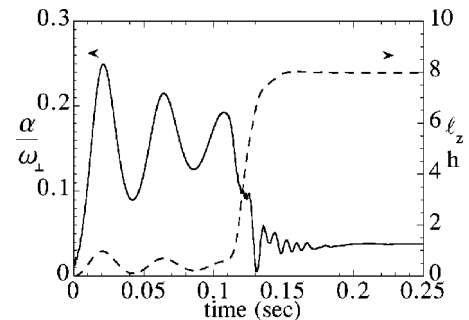

FIG. 3. Time evolution of the distortion parameter α (solid line) and the angular momentum $\ell_z/\hbar$ per atom (dashed line) corresponding to the dynamics of Fig. 1.

vortices are repelled and escape to the outside. Remarkably, the phase profile of Fig. 2(b) reveals that the repelled vortices also form a lattice on the outskirts of the condensate. Since they cannot be seen in the corresponding density profile of Fig. 1(f), they may be called "ghost" vortices.

The distortion of the condensate to an elliptic cloud was theoretically studied by Recati *et al.* [7]. Assuming the quadrupolar velocity field $\mathbf{v}(\mathbf{r}) = \alpha \nabla(xy)$, they obtained the distortion parameter $\alpha = \Omega(R_x^2 - R_y^2)/(R_x^2 + R_y^2)$ in the steady states as a function of Ω, where R_x and R_y are the sizes of the condensate along each direction. Madison *et al.* observed that, after the rotation of $\Omega = 0.7\omega_\perp$ starts suddenly, α oscillates during a few hundred milliseconds and then falls abruptly to a value below 0.1 when vortices enter the condensate from its boundary surface [6]. Figure 3 shows the oscillation of α and the increase of the angular momentum $\ell_z/\hbar$ per atom in our dynamics of Fig. 1. This figure closely resembles Fig. 3 of Ref. [6], and our scenario is thus consistent with the experimental results.

The dispersion relation of the surface waves [16] of a rotating condensate is obtained as follows. The substitution of the Madelung transformation $\psi = |\psi| e^{i\theta}$ into Eq. (1) yields

$$\frac{\partial |\psi|^2}{\partial t} + \nabla \cdot [|\psi|^2 (\mathbf{v} - \Omega \times \mathbf{r})] = 0, \tag{3a}$$

$$m \frac{\partial \mathbf{v}}{\partial t} = -\nabla \left\{ \delta\mu + \frac{m}{2}(\mathbf{v} - \Omega \times \mathbf{r})^2 - \frac{m}{2}\Omega^2 r^2 \right\}, \tag{3b}$$

where $\mathbf{v} = (\hbar/m)\nabla\theta$ and $\delta\mu = V_{\text{tr}} + g|\psi|^2 - \hbar^2/2m|\psi|\nabla^2|\psi| - \mu$. By linearizing Eq. (3), we obtain the dispersion relation of the surface waves $\omega^2 = R(\omega_\perp^2 - \Omega^2)k$ with the condensate size R. The dependence of ω on R shows that the surface with lower curvature is excited more easily, which is clearly seen in Fig. 1. The group velocity $d\omega/dk = \sqrt{R(\omega_\perp^2 - \Omega^2)}/(2\sqrt{k})$ agrees with the propagation velocity of the surface wave in our simulation. As discussed by Al Khawaja *et al.* [16], the surface waves are connected with the low-energy excitations studied by Stringari and Dalfovo *et al.* [17], and Isoshima and Machida [10].

We have examined the critical frequency at which vortices can enter with $C = 420$ corresponding to the experimental condition [4], and found that only when Ω is larger than $\Omega_{c1} \simeq 0.57\omega_\perp$, can vortices enter the condensate and form a lattice. This critical frequency is closer to the observed value $\Omega_{\text{nuc}} = 0.65\omega_\perp$, than the values obtained in previous literature. The critical frequencies have been studied from thermodynamic or stability arguments [10,11,18], but they are generally much smaller than the observed value. It should be noted that these critical frequencies only give the necessary condition which enables a vortex to exist stably at the center of the trap. Actually, vortices should be nucleated at the boundaries and come into the condensate; the condition of Ω, which realizes such nonlinear dynamics, may be generally different from that obtained from the stability arguments. Isoshima and Machida examined the local instability of nonvortex states toward vortex states within the Bogoliubov theory [10]. They note that this local instability could give
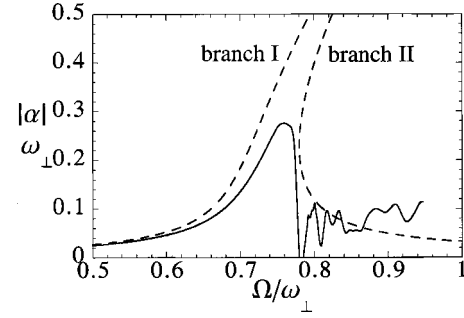

FIG. 4. Development of α for the ascending frequency $\Omega(t)$. The solid curve describes our numerical result, while the dashed curve represents the stationary nonvortex state obtained by Recati *et al.* [7]. See the text for more details.

higher critical frequencies than the global instability, which comes from comparing their total energy, for example, about $0.6\omega_\perp$ for the ENS experimental condition [19]. The stability analysis cannot answer what happens when the system goes over the linear region. Our paper reveals the importance of the nonlinear dynamics beyond the stability analysis. The detailed studies of the dependence of the number of vortices on Ω, that of Ω_{c1} on the number of condensate atoms [10], will be reported elsewhere.

Finally, we study the evolution of the condensate in a potential rotating with a time-dependent frequency $\Omega(t)$. The experiments were made by Madison *et al.* [6]. The condensate at every moment was in a stationary state with an elliptic cloud obtained by Recati *et al.* under the Thomas-Fermi limit [7], since the time dependence was slow enough. One of the important observations was that, for an ascending ramp, the condensate follows branch I of the nonvortex state until $\Omega_c \simeq 0.75\omega_\perp$. Beyond this critical frequency, the condensate changes from branch I to the more axisymmetric state, nucleating vortices. This critical frequency agrees with the frequency at which branch I becomes dynamically unstable [8]; however, the detailed nature of the bifurcation has remained to be clarified. We study the response of the condensate of $C = 420$ for the ascending frequency $\Omega(t) = ct$ with $c = 2\pi \times 400$ Hz/s; they are about the same values as those used in the ENS experiment. The obtained results are consistent with the experimental ones, as shown in Fig. 4. As Ω increases, the condensate becomes gradually elliptic following branch I, when the nucleated "ghost" vortices come to the surface of the condensate. When Ω is raised to the critical value $\Omega_{c2} \simeq 0.75\omega_\perp$, the vortices jostle with each other and excite the surface waves, reflecting the dynamical instability. Then, similar to the first set of calculations, some vortices enter the condensate, form a lattice and increase the angular momentum, while the condensate recovers the axisymmetry apart from branch I. The small discrepancy of the trace of our calculation from branch I in Fig. 4 may be attributed to a deviation from the Thomas-Fermi limit; the similar discrepancy is reported by Madison *et al.*, too [6].

It is necessary to compare two critical frequencies $\Omega_{c1} \simeq 0.57\omega_\perp$ and $\Omega_{c2} \simeq 0.75\omega_\perp$. What causes the difference? In the first set of calculations where the potential begins to rotate abruptly with a frequency Ω, the condensate first devi-

ates much from the stationary state $\alpha(\Omega)$ with the quadrupolar velocity field. As shown in Fig. 3, it seemingly relaxes to that state through the damped oscillation of the large amplitude, but it changes on the way to another state with a vortex lattice which has lower energy than the nonvortex state $\alpha(\Omega)$. The critical frequency Ω_{c1} means that the state with vortices can be realized dynamically from the nonvortex state only when $\Omega > \Omega_{c1}$. In the second calculation, as Ω increases slowly, the condensate follows quasistatically the nonvortex state $\alpha(\Omega)$ of branch I, even after it becomes metastable for $\Omega > \Omega_{c1}$. Only when Ω exceeds Ω_{c2}, the condensate can change from this state to the vortex state, reflecting the dynamical instability [8].

Recently García-Ripoll *et al.* and Feder *et al.* study this system by three-dimensional analysis of the GPE [18], taking account of the bending of vortex lines in the cigar-shaped potential. A bent vortex moves with the self-induced velocity proportional to its curvature [1], which is lacking in the two-dimensional dynamics. However, due to the high anisotropy of the cigar-shaped potential, vortices are aligned almost straight along the symmetry axis. It is therefore unlikely that the bending effect alters the results of our work qualitatively and significantly.

In conclusion, we have studied the dynamics of vortex lattice formation of a rotating trapped BEC by numerically solving the two-dimensional GPE, and obtained the following physical picture. When the trapping potential begins to rotate at a sufficiently fast frequency, the condensate is distorted to an elliptic shape and oscillates. Then, its boundary surface becomes unstable, exciting surface waves. The origin of these ripples is identified to be the interference of violent phase fluctuations that occur on the outskirts of the condensate; and some of the surface ripples develop into the vortex cores which then form a vortex lattice. The critical frequency for this process is found to be $\Omega_{c1} \simeq 0.57\omega_\perp$ for the condition at the ENS group. On the other hand, if the rotation frequency is raised slowly from zero, the condensate becomes elliptic and follows the nonvortex elliptic state with the quadrupolar flow [7]. When Ω exceeds $\Omega_{c2} \simeq 0.75\omega_\perp$, the condensate deviates from the state, nucleating vortices via the dynamical instability [8]. The whole dynamics is concerned with the "ghost" vortices, which are the phase defects outside the condensate. The obtained results are consistent with the experimental results of the ENS group [4,6].

[1] R. J. Donnelly, *Quantized Vortices in Helium II* (Cambridge University Press, Cambridge, 1991).

[2] L. M. Pismen, *Vortices in Nonlinear Fields* (Oxford University Press, Oxford, 1999).

[3] M. R. Matthews *et al.*, Phys. Rev. Lett. **83**, 2498 (1999).

[4] K. W. Madison *et al.*, Phys. Rev. Lett. **84**, 806 (2000).

[5] J. R. Abo-Shaeer *et al.*, Science **292**, 476 (2001).

[6] K. W. Madison *et al.*, Phys. Rev. Lett. **86**, 4443 (2001).

[7] A. Recati, F. Zambelli, and S. Stringari, Phys. Rev. Lett. **86**, 377 (2001).

[8] S. Sinha and Y. Castin, Phys. Rev. Lett. **87**, 190402 (2001).

[9] F. Chevy *et al.*, Phys. Rev. Lett. **85**, 2223 (2000).

[10] T. Isoshima and K. Machida, J. Phys. Soc. Jpn. **68**, 487 (1999); Phys. Rev. A **60**, 3313 (1999).

[11] G. Baym *et al.*, Phys. Rev. Lett. **76**, 6 (1996); F. Dalfovo *et al.*, Phys. Rev. A **53**, 2477 (1996); S. Sinha *ibid.* **55**, 4325 (1997); E. Lundth *et al.*, *ibid.* **55**, 2126 (1997); A. A. Svidzinsky *et al.*, Phys. Rev. Lett. **84**, 5919 (2000); Y. Castin *et al.*, Eur. Phys. J. D **7**, 399 (1999); F. Dalfovo *et al.*, Phys. Rev. A **63**, 011601(R) (2001).

[12] D. S. Jin *et al.*, Phys. Rev. Lett. **77**, 420 (1996); M.-O. Mewes *et al.*, *ibid.* **77**, 988 (1996).

[13] S. Choi, S. A. Morgan, and K. Burnett, Phys. Rev. A **57**, 4057 (1998).

[14] L. J. Campbell and R. M. Ziff, Phys. Rev. B **20**, 1886 (1979); M. Tsubota and H. Yoneda, J. Low Temp. Phys. **101**, 815 (1995).

[15] You can see the animation of this dynamics in http://matter.sci.osaka-cu.ac.jp/bsr/vortexex-e.html

[16] U. Al Khawaja, C. J. Pethick, and H. Smith, Phys. Rev. A **60**, 1507 (1999).

[17] S. Stringari, Phys. Rev. Lett. **77**, 2360 (1996); F. Dalfovo *et al.*, Phys. Rev. A **56**, 3840 (1997).

[18] J. J. García-Ripoll *et al.*, Phys. Rev. A **63**, 041603 (2001); D. L. Feder *et al.*, Phys. Rev. Lett. **86**, 564 (2001).

[19] K. Machida (private communication).